

Investigation of temperature dependence of microfibre coil resonators

Yu Yin, Jibo Yu, Yuxuan Jiang, Shi Li, Jing Ren, Gerald Farrell, Elfed Lewis, *Senior Member, IEEE*, and Pengfei Wang

Abstract—The temperature-sensitive performance of a microfibre coil resonator (MCR) is thoroughly investigated. The MCR is fabricated by wrapping a microfibre on a PMMA rod coated with a UV-curable low refractive index epoxy. The temperature sensitivity is measured by investigating the correlation between the shift of the resonant wavelength and the surrounding temperature. It is determined that a range of parameters of the MCRs, including the gap between two adjacent rings, the diameter of the supporting rod, the number of rings, and the diameter of the microfibre have a great influence on the temperature sensitivity of the MCRs. By optimizing the fabrication parameters of MCRs, such as the gap of the adjacent microrings and the diameter of supporting rod etc, the maximum temperature sensitivity obtained is 237.31 pm/°C, which is about 2.3 times higher than that of MCR embedded in EFIRON UV-373 polymer and 23 times higher than that of MCR embedded in Teflon because of the strong thermo-optic and thermal expansion effects of the low refractive index epoxy and the supporting rod used in the experiments. Theoretical (numerical) simulation and experiment results are considered in the assessment of the optical performance improvement of MCR-based optical fibre temperature sensors.

Index Terms—microfibre coil resonator, temperature sensitivity, fabrication parameters

I. INTRODUCTION

IN recent years, optical microfibres have attracted much attention in various application areas, including optical sensors, optical communications, and spectroscopy systems, thanks to their many advantages including compact structure, low loss, high evanescent field coupling, and sensitivity [1-4]. Optical devices based on microfibres are especially useful for sensing applications [5, 6]. Several systems based on microfibres have been considered as temperature sensors, such as microfibre resonators [7, 8], tapered microfibres [9, 10], fibre

Bragg gratings [11, 12], fibre couplers [13], and Fabry-Perot interferometers [14]. The microfibre resonators are highly sensitive to their surroundings because of the extremely large evanescent field associated with them [15], and this coupled with the resulting high quality factor of the resonant devices [16-19] has resulted in increasing research attention. Microfibre resonators can be divided into three types: loop [16], knot [17], and coil, respectively [18]. Among them, microfibre coil resonators (MCRs) are the most complex in construction, yet the only resonators with a three-dimensional (3D) structure. MCRs were initially proposed in 2004 [19] and experimentally demonstrated in 2007 [6]. While the loop and knot resonators have a relatively short coupling length for, the coupling in MCRs occurs along a much longer length of coils between the separate turns. MCRs can be used in sensors for biochemical applications, refractive index, electrical current, rotation, and temperature measurements [20-23]. As temperature sensors, MCRs can measure the temperature of the surrounding environment directly, and have a high sensitivity and relatively fast response times compared to other fibre optic temperature sensors such as Mach-Zehnder interferometer [24] and long period fibre-grating sensors [25]. For MCRs embedded in Teflon, the temperature sensitivity is about 10 pm/°C [26], and when they are embedded in EFIRON UV-373 polymer [27], the temperature sensitivity increases to about 100 pm/°C. However, the relationships between temperature sensitivities and different parameters including the gap between two adjacent rings, the diameter of the support rod, the number of rings, and the diameter of the microfibres of MCRs have not yet been fully investigated.

In this work, a new type of MCR was fabricated by wrapping a microfibre on a PMMA rod covered with a low refractive index epoxy. A comprehensive investigation on the temperature sensitivity of the MCRs was carried out. Our results show that the temperature sensitivity of the MCRs strongly depends on

This work was supported by the National Natural Science Foundation of China (NSFC) under grant 61575050, National Key R&D Program of China under grant 2016YFE0126500, Key Program for Natural Science Foundation of Heilongjiang Province of China under grant ZD2016012, the Open Fund of the State Key Laboratory on Integrated Optoelectronics (Grant no.: IOSKL2016KF03), this work was also supported by the 111 project (B13015) to the Harbin Engineering University and the Recruitment Program for Young Professionals (The Young Thousand Talents Plan). (Corresponding author: Pengfei Wang)

Yu Yin, Jibo Yu, Yuxuan Jiang, Shi Li, Jing Ren and Pengfei Wang are with the Key Laboratory of In-fiber Integrated Optics of Ministry of Education, College of Science, Harbin Engineering University, Harbin 150001, China (e-

mail: cbyy@hrbeu.edu.cn; yu20131164@hrbeu.edu.cn; merak@hrbeu.edu.cn; m18204313488@163.com; ren.jing@hrbeu.edu.cn; pengfei.wang@dit.ie). Pengfei Wang is also with the Key Laboratory of Optoelectronic Devices and Systems of Ministry of Education and Guangdong Province, College of Optoelectronic Engineering, Shenzhen University, Shenzhen, 518060, China (e-mail: pengfei.wang@dit.ie).

Gerald Farrell is with Photonics Research Centre, Dublin Institute of Technology, Kevin Street, Dublin 8, Ireland (e-mail: gerald.farrell@dit.ie).

Elfed Lewis is with Optical Fibre Sensors Research Centre, Department of Electronic and Computer Engineering, University of Limerick, Limerick, Ireland (e-mail: Elfed.lewis@ul.ie).

the gap between two adjacent rings, the diameter of the supporting rod, the number of rings, and the diameter of the microfibres. The proposed MCRs show great potential in temperature sensing applications. The sensitivity can be further improved by optimizing the parameters of the MCRs with respect to the present experimental results.

II. THEORETICAL ANALYSIS

According to the theoretical analysis proposed by Sumetsky [28], the light propagation along a MCR with n turns is described by the following equations:

$$\begin{cases} \frac{dA_1}{ds} = kA_2 \\ \frac{dA_i}{ds} = k(A_{i-1} + A_{i+1}) \\ \frac{dA_n}{ds} = kA_{n-1} \end{cases} \quad (1)$$

where $A_i(s)$ is the amplitude of the electric field in the i th coil, the variable s is the distance the light has propagated round the coil (along the optical axis) and k is the coupling coefficient between two adjacent coils. The coefficient S is the length of the coil, so $0 < s < S$. In addition to (1), the continuity condition at the end of each coil can be given by the equation:

$$A_{i+1}(0) = A_i(S) \exp(i\beta S) \quad (2)$$

where $A_{i+1}(0)$ is the input amplitude at the beginning of the $i+1$ th coil and $A_i(S)$ is the output amplitude at the end of the i th coil. β is the propagation constant for the microfibre. According to (2), the input of the MCR is $A_1(0)$ while the output of the MCR is $A_n(S) \exp(i\beta S)$. The transmission coefficient is thus defined as:

$$T = A_n \exp(i\beta S) / A_1(0) \quad (3)$$

Based on (3), the calculated transmission spectrum of a MCR is shown in Fig. 1 with 4 coils and with $k = 5.66 \text{ mm}^{-1}$, $S = 2.52\pi \text{ mm}$ and the optical loss coefficient $\alpha = 0.054 / \text{mm}$ using the complex propagation constant $\beta = 2\pi/\lambda + i\alpha$.

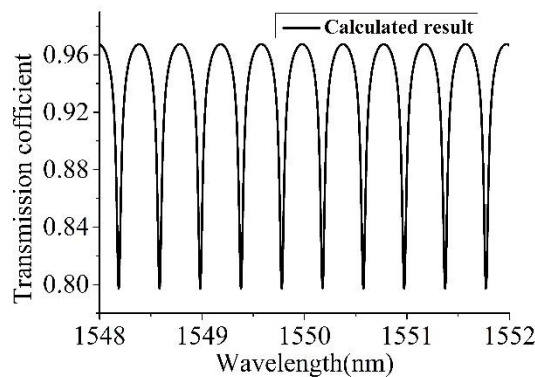


Fig. 1. Calculated transmission spectrum of a MCR with four turns.

MCRs can be relatively easily applied to temperature sensing due to the presence of the thermo-optic and thermal expansion effects [26]. The resonance wavelength moves towards the longer wavelength (red shift) with increasing temperature when the positive thermo-optic effect of the microfibre prevails over the negative thermo-optic effect of the low refractive index epoxy, and moves towards the shorter wavelength (blue shift) with decreasing temperature [29]. In MCRs, the microfibre

transmits more light in the low refractive index epoxy as a result of the strong evanescent field effect. Therefore the resonant wavelength is subjected to a red shift.

The temperature dependence of a MCR embedded in a low refractive index epoxy can be given by the following equations [30]:

$$S = \frac{d\lambda_r}{dT} = S_{TOM} + S_{TOL} + S_{TEM} + S_{TEL} \quad (4)$$

$$\begin{cases} S_{TOM} = \frac{\lambda_r}{n_{eff}} \sigma_M \frac{\partial n_{eff}}{\partial n_M} \\ S_{TOL} = \frac{\lambda_r}{n_{eff}} \sigma_L \frac{\partial n_{eff}}{\partial n_L} \\ S_{TEM} = \frac{\lambda_r}{n_{eff}} \alpha_M (n_{eff} + r \frac{\partial n_{eff}}{\partial r}) \\ S_{TEL} = \gamma \alpha_L \lambda_r \end{cases} \quad (5)$$

where n_{eff} is the effective refractive index, λ_r is the resonance wavelength, and r is the radius of the microfibre, respectively. Different values of S represent contributions to the temperature sensitivity arising respectively from the thermo-optic effects of the microfibre (TOM) and the low refractive index epoxy (TOL), the thermal expansion effect of the microfibre (TEM), and the thermal expansion effects of the low refractive index epoxy and the supporting rod (TEL). α_M is the thermal expansion coefficient of the microfibre and α_L is the general thermal expansion coefficient of the low refractive index epoxy and the supporting rod. σ_M and σ_L are the thermo-optic coefficients of the microfibre and the low refractive index epoxy. For the silica microfibre, $\alpha_M = 5.5 \times 10^{-7} / ^\circ\text{C}$ and $\sigma_M = 1.1 \times 10^{-5} / ^\circ\text{C}$ [26]. For the supporting rod (PMMA), $\alpha_P \approx 0.8 \times 10^{-4} / ^\circ\text{C}$, $\sigma_P \approx -1.1 \times 10^{-4} / ^\circ\text{C}$ [31] and for the low refractive index epoxy used in this experiment, $\alpha_L \approx 1.7 \times 10^{-4} / ^\circ\text{C}$, $\sigma_L \approx -1.1 \times 10^{-4} / ^\circ\text{C}$ [32]. Because of the mismatch between the thermal expansion coefficients of the microfibre, the supporting rod and the low refractive index epoxy, a coefficient γ in S_{TEL} was defined to represent the effective influence on the length of coil due to the thermal expansion effects of the low refractive index epoxy and the supporting rod [33].

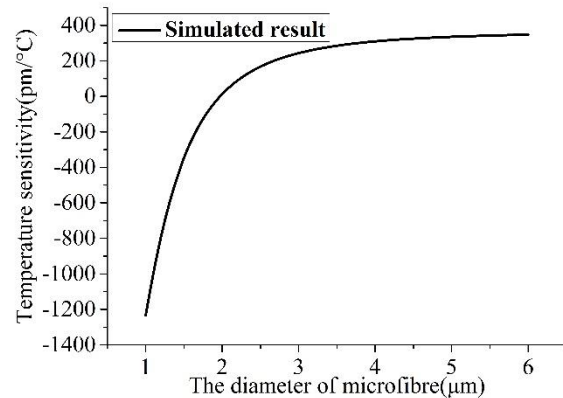


Fig. 2. Simulated temperature sensitivity dependence on microfibre diameter.

Fig. 2 shows the relationship of the calculated temperature sensitivity and diameter of the microfibre using the following parameters: the refractive index of the microfibre is 1.4443, the refractive index of the low refractive index epoxy is 1.32 and the resonance wavelength is at 1550 nm. In the analysis, S_{TEL} is

fixed at a constant value. As shown in Fig. 2, when the microfibre diameter changes from 1 to 3 μm , the temperature sensitivity increases dramatically with microfibre diameter but when the microfibre diameter is larger than 3 μm , the temperature sensitivity only increases slowly and approaches a constant value. The reason is that the microfibre and the low refractive index epoxy show conflicting thermal-optic responses due to the opposite slope of their thermo-optic coefficients. When the microfibre diameter is small (e.g., $\leq 3 \mu\text{m}$), the thermo-optic effect of the microfibre has a dominating influence on the temperature sensitivity due to the strong evanescent field effect. As the microfibre diameter increases, the negative thermo-optic effect of the low refractive index epoxy begins to play a commensurately important role, which leads to the leveling off in the change of the temperature sensitivity with temperature.

III. MCR FABRICATION AND EXPERIMENTAL SETUP

The manufacture of MCRs can be separated into three steps as shown in Fig. 3 [34]: (1) first a microfibre was fabricated and fixed on a rotating stage; (2) the microfibre was wrapped on a PMMA rod by the combination of a rotating stage and a linear stage. The PMMA rod was covered with a UV-curable low refractive index epoxy; (3) and the fabricated MCR was packaged with the same low refractive index epoxy and fixed on a slide glass using the same low refractive index epoxy.

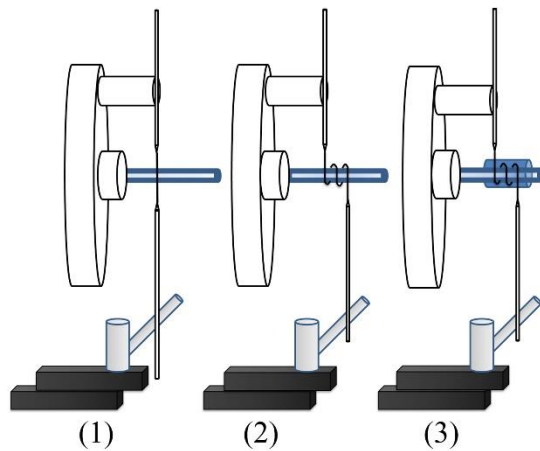


Fig. 3. Schematic of the fabrication processes of MCRs.

The fabrication processes is described in detail as follows:

In the first step, a conventional single-mode fibre (Coring SMF-28) was heated using a ceramic heat emitter and tapered down to microfibre dimensions [35]. The diameter of the microfibre can be reliably tuned from 1 μm to 10 μm and the length of the waist region can be adjusted from 13 mm to 16 mm. In the second step, to fabricate the MCR-based temperature sensor, the microfibre was wrapped around a supporting rod and the gap between two adjacent rings was accurately varied using a rotation stage controlled by a computer. Because of the unwanted loss resulting from the different refractive indices between the PMMA and the microfibre, the surface of the PMMA rod was covered with a UV-curable low refractive index epoxy and fully cured using a

UV lamp. In the final step, the MCR was packaged with the same UV-curable low refractive index epoxy and removed from the rotating stage after the epoxy was completely solidified. The fabricated MCR was placed on a glass slide coated with the same UV-curable low refractive index epoxy to maintain mechanical stability for subsequent measurements. For the temperature sensitivity measurement, the fabricated MCR was placed inside a temperature-controlled environment chamber (ESPEC SH-222), the input fibre was connected to a broadband amplified spontaneous emission (ASE) source (YSL SC-series) and the output fibre was connected to an optical spectrum analyzer (OSA) (YOKOGAWA, AQ-6370C) [36], as shown in Figure 4.

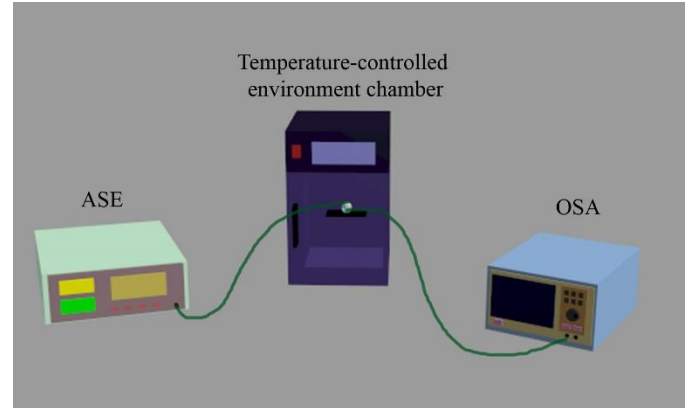


Fig. 4. Schematic of experimental set-ups for the temperature sensitivity measurement.

IV. ANALYSIS AND DISCUSSION

By utilizing the fabrication method mentioned above, several MCRs were fabricated with varying parameters, including different gap lengths between adjacent rings, diameters of the supporting rod, the number of rings, and diameters of the microfibres. Fig. 5(a) shows a typical transmission spectrum of an MCR with a gap of 5.43 μm between adjacent rings, a supporting rod diameter of 1.26 mm, the number of rings of 4, and a microfibre diameter of 2.24 μm . Fig. 5(b) shows a microscope picture of the fabricated MCR.

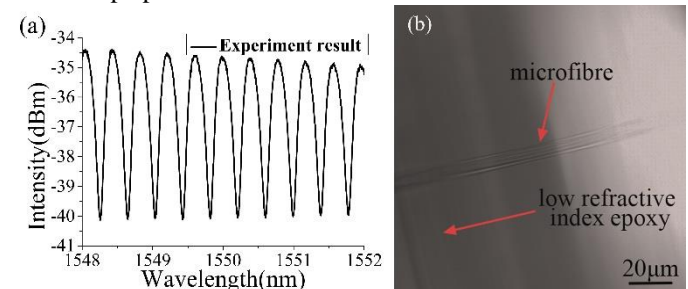


Fig. 5. (a) Measured transmission spectrum of MCR (b) Microscope image of the fabricated MCR before packaged by the low refractive index epoxy.

As shown in Fig. 5(a), the free spectral range (FSR) and the full width at half maximum ($FWHM$) of the fabricated MCR are 389.93 pm and 257.37 pm, respectively. Based on this, the Q-factor (Q) and the finesse (F) can be calculated as:

$$Q = \frac{\lambda}{FWHM} \quad (6)$$

$$F = \frac{FSR}{FWHM} \quad (7)$$

The Q-factor (Q) and the finesse (F) were found to be 6022.46 and 1.52, respectively.

Fig. 6(a) shows the resonant spectra of MCRs measured at different temperatures. The environmental temperature was changed from 21 °C to 23 °C and the spectra were recorded for temperature increments of 1 °C. As shown in Fig. 6(a), the resonance wavelength moves towards long wavelengths as the temperature increases. The experimental result coincides with the theoretical analysis mentioned above.

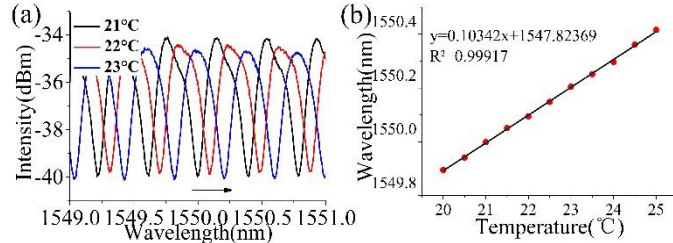


Fig. 6. (a) Resonant spectra of MCRs measured at different temperatures (b) Temperature dependence of the resonance wavelength. The solid line is the linear fit to the experimental data (solid squares).

Fig. 6(b) shows variation of resonance wavelength as a function of temperature in the range of from 20 °C to 25 °C, and the spectra were recorded for temperature increments of 0.5 °C. It is clearly shown that the resonance wavelength can be fitted to a linear regression. The temperature sensitivity of the studied MCR is ~ 103.42 pm/°C, which is considerably higher than that of MCRs embedded in Teflon previously reported. The greater thermo-optic and thermal expansion effects of the low index refractive epoxy and the supporting rod employed in this work account for the enhanced temperature sensitivity.

The response time of the studied MCR is also measured. The studied MCR is fixed and heated by the temperature-controlled environment chamber (ESPEC SH-222). A schematic of the temporal response experiment is shown as Fig. 7(a). A tunable laser (Santec TSI-710) was tuned to 1550nm, and the temperature was increased to 25 °C using the temperature-controlled environment chamber. The door of temperature-controlled environment chamber was opened to lower the temperature to the general room temperature and the time dependence of the temperature measurement was measured using the oscilloscope (Tektronix MDO4054-6, 5 GHz/s), as shown in Fig. 7(b). For the studied MCR, the measured response time is about 317.41ms.

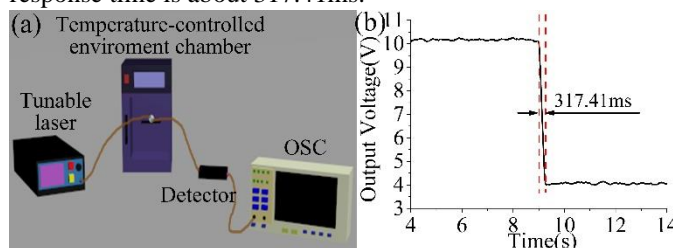


Fig. 7. (a) Schematic of experimental set-ups for the response time measurement (b) Measurement of response time of studied MCR.

A systematic investigation has been carried out on the influence on a MCR-based temperature sensor of changes to including the gap between adjacent rings, the diameter of the supporting rod, the number of rings, and the diameter of the microfiber. The results are of this investigation are discussed below.

Fig. 8(a) shows the resonance wavelength shift of MCRs with different gaps between adjacent rings in the temperature range from 20 °C to 25 °C. The supporting rod diameter, the number of rings, and the diameter of the microfiber were fixed at 1.26 mm, 4, and 2.24 μ m, respectively. The gap between adjacent rings was selected to be 2.83, 3.53, 4.25, 5.43, and 6.23 μ m. The temperature sensitivity of the MCRs was obtained using linear fitting to the experimental data.

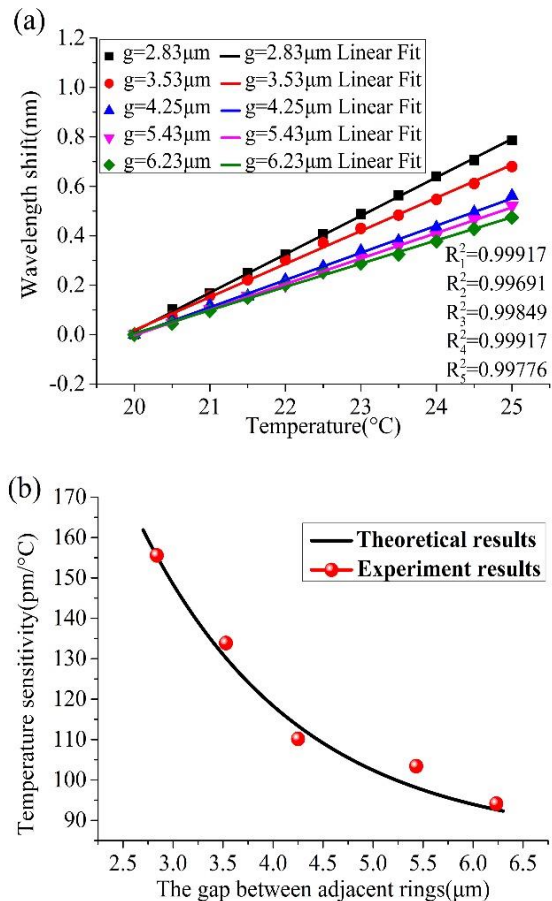


Fig. 8. (a) Temperature dependence of the resonance wavelength for MCRs with different gaps between adjacent rings. The lines are linear fits to the experimental data (solid points) (b) Variation of temperature sensitivity with the gaps between adjacent rings. The points are experimental data, and the line represents the theoretically calculated results.

As shown in Fig. 8(b), the temperature sensitivity decreases from 155.58 to 94.12 pm/°C with increasing gap length between adjacent rings, which is in agreement with the theoretical results from Equations (1) to (3). According to the theoretical analysis, the coupling coefficient k decreases as the gap between adjacent rings increases, and this is responsible for the corresponding decrease in temperature sensitivity of the MCRs.

Fig. 9(a) shows the resonance wavelength shift of MCRs with different supporting rod diameters in the temperature range of from 20 °C to 25 °C. The gap between adjacent rings, the number of rings, and the diameter of the microfiber were fixed at 5.43 μ m, 4, and 2.24 μ m, respectively. By changing the thickness of the low refractive index epoxy, the diameter of the supporting rod was set to be 1.21, 1.26, 1.31, 1.35, and 1.41 mm. The temperature sensitivity was obtained using linear fitting to the experimental data.

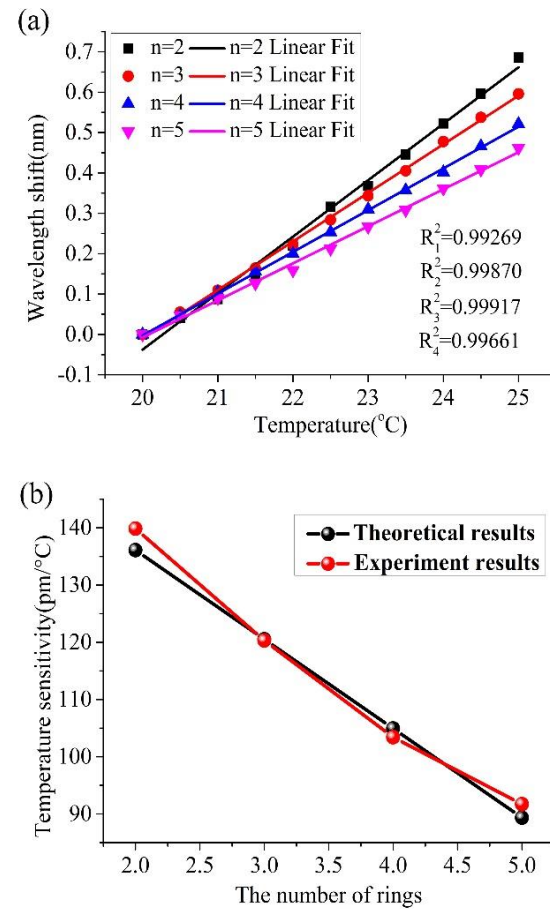
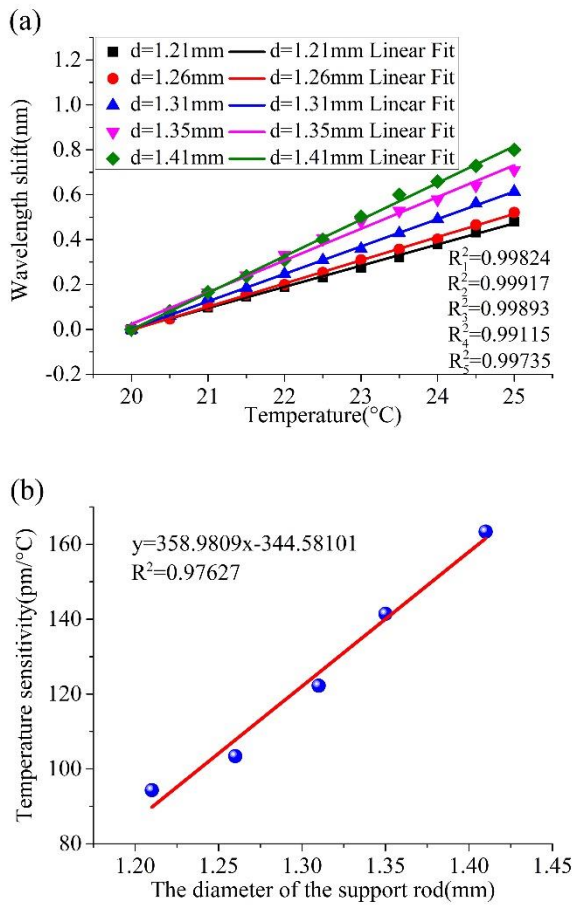


Fig. 9. (a) Temperature dependence of the resonance wavelength for MCRs with different supporting rod diameters. The lines are linear fits to the experimental data (solid points); (b) Variation of temperature sensitivity with diameter of the supporting rod. The solid line is the linear fit to the temperature sensitivity (solid points).

As shown in Fig. 9(b), the temperature sensitivity increases from 94.12 to 163.4 pm/°C with increasing diameter of the supporting rod. Clearly, the microfibre coil length increases with increasing supporting rod diameter. The increase in the coil length leads to enhanced coupling interaction between adjacent coils, as a result, the temperature sensitivity of the MCRs increases.

Fig. 10(a) shows the resonance wavelength shift of MCRs with different numbers of rings in the temperature range from 20 °C to 25 °C. The gap between adjacent rings, the diameter of supporting rod, and the diameter of the microfibre were fixed at 5.43 μm , 1.26 mm, and 2.24 μm , respectively. The number of rings was changed from 2 to 5. The temperature sensitivity was obtained using linear fitting to the experimental data.

Fig. 10. (a) Temperature dependence of the resonance wavelength for MCRs with different number of rings. The lines are linear fits to the experimental data (solid points); (b) Variation of temperature sensitivity with the number of rings. The points are experimental data, and the line represents the theoretically calculated results.

As shown in Fig. 10(b), the temperature sensitivity of the MCRs decreases from 139.86 to 91.72 pm/°C with increasing numbers of rings, which is in agreement with the theoretical results from Equations (1) to (3). According to the theoretical analysis, varying the number of rings can change the transmission characteristics of the MCRs, as a result, the temperature sensitivity of the MCRs changes with the number of rings.

Fig. 11(a) shows the resonance wavelength shift of MCRs with different microfibre diameters in the temperature range from 20 °C to 25 °C. The gap between adjacent rings, the diameter of the supporting rod, and the number of rings were fixed at 5.43 μm , 1.26 mm, and 4, respectively. The diameter of the microfibres was selected at fixed values in the range 2.13, 2.24, 2.39, 2.52, 2.76, and 2.96 μm . The temperature sensitivity was obtained using linear fitting to the experimental data.

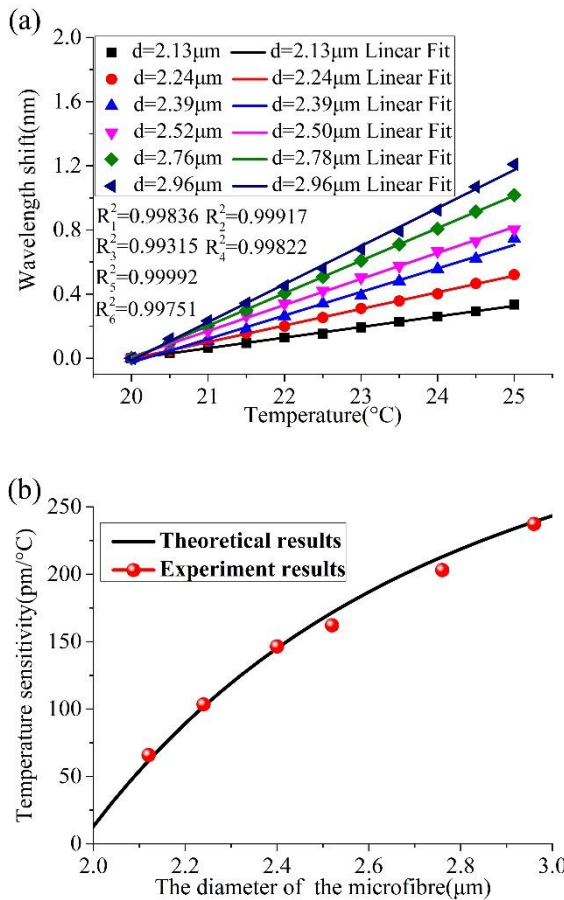


Fig. 11. (a) Temperature dependence of the resonance wavelength for MCRs with different microfibre diameter. The lines are linear fits to the experimental data (solid points); (b) Variation of temperature sensitivity with the diameter of the microfibre. The points are experimental data, and the line represents the theoretically calculated results as shown in Fig. 2.

As shown in Fig. 11(b), the temperature sensitivity of the MCRs increases from 65.85 to 237.31 pm/°C with increasing diameter of the microfibre, which is in agreement with the simulated results of Figure 2. The discrepancies between the simulated and experimental data are due to the fact that it is impossible to control all the parameters of the MCRs with complete accuracy and consistently (repeatability). The limitation on repeatability is due to the fact that the experimental parameters e.g. thickness of the depth of adhesive, separation of the coils etc. cannot be accurately controlled or predetermined and in some cases can only be measured with limited accuracy following fabrication. Table I summarises the difference between the simulated and experimentally measured parameters and also the experimental error between the simulated and experimental data.

TABLE I
THE DIFFERENCE BETWEEN PROSPECT AND MEASUREMENT AND EXPERIMENTAL ERROR BETWEEN THE SIMULATED AND EXPERIMENTAL RESULTS

Fibre diameter	The thickness of depth of adhesive	The separation of the coils	The difference from thickness of depth of adhesive	The difference from separation of the coils	The experimental error
2.13μm	1.27mm	5.43μm	0.79%	0%	6.39%
2.24μm	1.26mm	5.68μm	0%	4.6%	1.56%
2.39μm	1.26mm	5.54μm	0%	2.03%	0.91%
2.52μm	1.24mm	5.43μm	1.58%	0%	5.79%
2.76μm	1.24mm	5.56μm	0.79%	2.39%	4.86%
2.96μm	1.26mm	5.60μm	0.79%	3.13%	0.68%

V. CONCLUSION

A temperature sensor based on MCRs has been successfully demonstrated yielding excellent temperature sensitivity from 87.34 to 237.31 pm/°C. The temperature sensitivity is estimated based on the resonance wavelength shift as a function of temperature. The relationships between the temperature sensitivity and the gap between adjacent rings, the supporting rod diameter, the number of rings, and the microfibre diameter have been investigated. The experimental results show that the temperature sensitivity of the MCRs increases as the gap between adjacent rings and the number of rings decrease, and as the diameters of the supporting rod, and the microfibre increase. Possible discrepancies between the calculated and experimental data arise because the MCRs are highly susceptible to the experimental parameters such as the supporting rod diameter and the microfibre diameter, the complete control of which is nearly impossible in this work. However, by optimizing the parameters of the MCRs, the maximum temperature sensitivity can be as high as 237.31 pm/°C, which is about 2.3 times higher than that of previously studied MCR structures embedded in EFIRON UV-373 polymer and 23 times higher than that of MCR embedded in Teflon. Such an enhanced sensitivity is due to the favorable contributions of the thermo-optic and thermal expansion effects related to the low refractive index epoxy and the supporting rod respectively which have been employed in this work. The studied MCRs have considerable merits including compact size, high sensitivity and a fast response time, and thus hold great potential in fabricating MCR-based temperature sensors.

REFERENCES

- [1] C. R. Liao, D. N. Wang, X. He, and M. W. Yang, "Twisted Optical Microfibers for Refractive Index Sensing," *IEEE Photonics Technology Letters*, vol. 23, no. 13, pp. 848-850, 2011.
- [2] P. Wang, G. Brambilla, M. Ding, Y. Semenova, Q. Wu, and G. Farrell, "High-sensitivity, evanescent field refractometric sensor based on a tapered, multimode fiber interference," *Optics Letters*, vol. 36, no. 12, p. 2233, 2011.
- [3] S. Wang, J. Wang, G. Li, and L. Tong, "Modeling optical microfiber loops for seawater sensing," *Applied Optics*, vol. 51, no. 15, p. 3017, 2012.

- [4] Y. Wu *et al.*, "Hybrid Graphene-Microfiber Waveguide for Chemical Gas Sensing," *IEEE Journal of Selected Topics in Quantum Electronics*, vol. 20, no. 1, pp. 49-54, 2013.
- [5] X. Jiang, Y. Chen, G. Vienne, and L. Tong, "All-fiber add-drop filters based on microfiber knot resonators," *Optics Letters*, vol. 32, no. 12, p. 1710, 2007.
- [6] F. Xu, P. Horak, and G. Brambilla, "Optical microfiber coil resonator refractometric sensor," *Optics Express*, vol. 15, no. 12, p. 7888, 2007.
- [7] Y. Wu, Y. J. Rao, Y. H. Chen, and Y. Gong, "Miniature fiber-optic temperature sensors based on silica/polymer microfiber knot resonators," *Optics Express*, vol. 17, no. 20, p. 18142, 2009.
- [8] G. Y. Chen, G. Brambilla, and T. P. Newson, "Inspection of electrical wires for insulation faults and current surges using sliding temperature sensor based on optical Microfibre coil resonator," *Electronics Letters*, vol. 49, no. 1, pp. 46-47, 2013.
- [9] J. L. Kou, J. Feng, L. Ye, F. Xu, and Y. Q. Lu, "Miniaturized fiber taper reflective interferometer for high temperature measurement," *Optics Express*, vol. 18, no. 13, pp. 14245-50, 2010.
- [10] M. Z. Muhammad, A. A. Jasim, H. Ahmad, H. Arof, and S. W. Harun, "Non-adiabatic silica microfiber for strain and temperature sensors," *Sensors & Actuators A Physical*, vol. 192, no. 4, pp. 130-132, 2013.
- [11] J. Kou, S. Qiu, F. Xu, and Y. Lu, "Demonstration of a compact temperature sensor based on first-order Bragg grating in a tapered fiber probe," *Optics Express*, vol. 19, no. 19, pp. 18452-7, 2011.
- [12] C. Ji, C. L. Zhao, J. Kang, X. Dong, and S. Jin, "Multiplex and simultaneous measurement of displacement and temperature using tapered fiber and fiber Bragg grating," *Review of Scientific Instruments*, vol. 83, no. 5, p. 053109, 2012.
- [13] M. Ding, P. Wang, and G. Brambilla, "A microfiber coupler tip thermometer," *Optics Express*, vol. 20, no. 5, p. 5402, 2012.
- [14] H. Y. Choi, K. S. Park, S. J. Park, U. C. Paek, B. H. Lee, and E. S. Choi, "Miniature Fabry-optic high temperature sensor based on a hybrid structured Fabry-Perot interferometer," *Optics Letters*, vol. 33, no. 21, p. 2455, 2008.
- [15] F. Xu and G. Brambilla, "Demonstration of a refractometric sensor based on optical microfiber coil resonator," *Applied Physics Letters*, vol. 92, no. 10, p. 5742, 2008.
- [16] T. Lee, N. G. R. Broderick, and G. Brambilla, "Resonantly enhanced third harmonic generation in microfiber loop resonators," *Optics Letters*, vol. 37, no. 24, pp. 5121-5123, 2013.
- [17] Y. Li, Z. Xu, Q. Sun, Y. Luo, L. Zhang, and D. Liu, "A single longitudinal mode fiber ring laser based on cascaded microfiber knots filter," *IEEE Photonics Technology Letters*, vol. 28, no. 20, pp. 2172-2175, 2016.
- [18] S. Yan, B. Zheng, J. Chen, F. Xu, and Y. Lu, "Optical electrical current sensor utilizing a graphene-microfiber-integrated coil resonator," *Applied Physics Letters*, vol. 42, no. 5, p. 57, 2015.
- [19] M. Sumetsky, "Optical fiber microcoil resonators," *Optics Express*, vol. 12, no. 10, p. 2303, 2004.
- [20] C. Y. Chao and L. J. Guo, "Design and optimization of microring resonators in biochemical sensing applications," *Journal of Lightwave Technology*, vol. 24, no. 3, pp. 1395-1402, 2006.
- [21] M. Belal, Z. Song, Y. Jung, G. Brambilla, and T. P. Newson, "Optical fiber microwire current sensor," *Optics Letters*, vol. 35, no. 18, p. 3045, 2010.
- [22] F. Xu and G. Brambilla, "Demonstration of a refractometric sensor based on optical microfiber coil resonator," in *Lasers and Electro-Optics, 2008 and 2008 Conference on Quantum Electronics and Laser Science. CLEO/QELS 2008. Conference on*, 2008, pp. 1-2.
- [23] J. Scheuer, "Fiber microcoil optical gyroscope," *Optics Letters*, vol. 34, no. 11, pp. 1630-2, 2009.
- [24] P. Lu, L. Men, K. Sooley, and Q. Chen, "Tapered fiber Mach-Zehnder interferometer for simultaneous measurement of refractive index and temperature," *Applied Physics Letters*, vol. 94, no. 13, pp. 131110-131110-3, 2009.
- [25] Y. P. Wang, L. Xiao, D. N. Wang, and W. Jin, "Highly sensitive long-period fiber-grating strain sensor with low temperature sensitivity," *Optics Letters*, vol. 31, no. 23, p. 3414, 2006.
- [26] Y. Chen, F. Xu, and Y. Q. Lu, "Teflon-coated microfiber resonator with weak temperature dependence," *Optics Express*, vol. 19, no. 23, pp. 22923-8, 2011.
- [27] G. Chen *et al.*, "Investigation of Thermal Effects on Embedded Microcoil Resonators," in *Lasers and Electro-Optics Europe*, 2011, pp. 1-1.
- [28] M. Sumetsky, "Uniform coil optical resonator and waveguide: transmission spectrum, eigenmodes, and dispersion relation," *Optics Express*, vol. 13, no. 11, pp. 4331-40, 2005.
- [29] H. Yang, S. Wang, X. Wang, J. Wang, and Y. Liao, "Temperature sensing in seawater based on microfiber knot resonator," *Sensors*, vol. 14, no. 10, p. 18515, 2014.
- [30] X. Zeng, Y. Wu, C. Hou, J. Bai, and G. Yang, "A temperature sensor based on optical microfiber knot resonator," *Optics Communications*, vol. 282, no. 18, pp. 3817-3819, 2009.
- [31] W. Zhang and D. J. Webb, "Factors influencing the temperature sensitivity of PMMA based optical fiber Bragg gratings," *Proceedings of SPIE - The International Society for Optical Engineering*, 2014.
- [32] Z. Zhang, P. Zhao, P. Lin, and F. Sun, "Thermo-optic coefficients of polymers for optical waveguide applications," *Polymer*, vol. 47, no. 14, pp. 4893-4896, 2006.
- [33] G. X. Li, J. Wang, H. J. Yang, and S. S. Wang, "Simulation study of microring resonator for seawater salinity sensing with weak temperature dependence," *European Physical Journal Applied Physics*, vol. 68, no. 2, 2014.
- [34] Q. Liu and Y. Chen, "PMMA-rod-assisted temperature sensor based on a two-turn thick-microfiber resonator," *Journal of Modern Optics*, vol. 63, no. 2, pp. 159-163, 2016.
- [35] Y. Chen, Y. Ming, W. Guo, F. Xu, and Y. Q. Lu, "Temperature characteristics of microfiber coil resonators embedded in Teflon," in *Communications and Photonics Conference and Exhibition, 2011. ACP. Asia*, 2012, pp. 1-6.
- [36] G. Y. Chen, T. Lee, X. L. Zhang, G. Brambilla, and T. P. Newson, "Temperature compensation techniques for resonantly enhanced sensors and devices based on optical microcoil resonators," *Optics Communications*, vol. 285, no. 23, pp. 4677-4683, 2012.